

OPEN

Dermatofibrosarcoma Protuberans: Computed Tomography and Magnetic Resonance Imaging Findings

Liang Zhang, MD, Qing-yu Liu, MD, Yun Cao, MD, Jin-shuang Zhong, MD, and Wei-dong Zhang, MD

Abstract: The aim of this study was to analyze the computed tomography (CT) and magnetic resonance imaging (MRI) findings of dermatofibrosarcoma protuberans (DFSP), with a view to improving the diagnosis of this kind of tumor.

A total of 27 cases of histopathologically confirmed DFSP were analyzed retrospectively. Of these, 18 patients underwent a CT scan and 9 patients underwent an MRI. All patients underwent unenhanced and contrast-enhanced examinations; 1 patient underwent multiphase CT enhancement examination. Imaging characteristics, including location, shape, size, number, edge, and attenuation or intensity of each lesion, both unenhanced and contrast enhanced, were analyzed.

Of the 27 cases, 24 were solitary, 2 had 2 nodules, and 1 had multiple confluent tumors. The lesion with multiple confluent tumors was ill defined and irregular; the other lesions were oval or round, well-defined nodules or masses. The unenhanced CT images showed 19 homogenous isodense lesions. There was no calcification in any of the patients. The contrast-enhanced CT images showed intermediate and marked non-homogeneous enhancement in 13 lesions, intermediate homogeneous enhancement in 4 lesions, and a mild heterogeneous enhancement in 2 lesions. MR T1-weighted images revealed 1 ill-defined and 9 well-defined homogeneous isointense lesions. T2-weighted images showed homogeneous hyperintensity to the muscles in 6 lesions, 3 mild hyperintense lesions with hypointense lesions, and 1 mixed, mild hyperintense and isointense lesion. Contrast-enhanced T1-weighted images demonstrated intermediate and marked nonhomogeneous enhancement in 9 lesions and intermediate homogeneous enhancement in 1 lesion.

DFSP is characterized by a subcutaneous well-defined soft tissue nodule or mass on plain CT/MR scans, and shows intermediate-to-marked enhancement on contrast-enhanced CT/MR scans. The imaging findings for DFSP are nonspecific, but may help to define the diagnosis in an appropriate clinical setting.

Editor: Ismael Maatouk.

Received: November 2, 2014; revised: April 24, 2015; accepted: May 20, 2015.

From the Department of Radiology (LZ, JZ, WZ), Collaborative Innovation Center for Cancer Medicine, State Key Laboratory of Oncology in South China, Sun Yat-sen University Cancer Center; Department of Radiology (QL), The Second Affiliated Hospital, Sun Yat-sen University; and Department of Pathology (YC), Collaborative Innovation Center for Cancer Medicine, State Key Laboratory of Oncology in South China, Sun Yat-sen University Cancer Center, Guangzhou, Guangdong, P.R. China.

Correspondence: Wei-dong Zhang, Department of Radiology, Collaborative Innovation Center for Cancer Medicine, State Key Laboratory of Oncology in South China, Sun Yat-sen University Cancer Center, 651 Dongfengdong Road, Guangzhou, Guangdong 510060, P.R. China (e-mail: dongw.z@163.com).

The authors have no funding and conflicts of interest to disclose.

Copyright © 2015 Wolters Kluwer Health, Inc. All rights reserved.

This is an open access article distributed under the Creative Commons Attribution-NonCommercial-NoDerivatives License 4.0, where it is permissible to download, share and reproduce the work in any medium, provided it is properly cited. The work cannot be changed in any way or used commercially.

ISSN: 0025-7974

DOI: 10.1097/MD.0000000000001001

(*Medicine* 94(24):e1001)

Abbreviations: CT = computed tomography, DFSP = dermatofibrosarcoma protuberans, H&E = hematoxylin and eosin, MRI = magnetic resonance imaging.

Dermatofibrosarcoma protuberans (DFSP) is a rare low-grade malignant cutaneous tumor. It was first reported by Darier and Ferrand and called “progressive and recurrent skin fibroma” in 1924.¹ In 1925, Hoffman named it as DFSP.² DFSP often occurs in the dermis and subcutaneous layers. Typical DFSP shows superficial skin nodules or masses, and often protrudes from the skin surface. DFSP is often misdiagnosed, especially for larger tumors with deep tissue invasion and atypical manifestations, which often results in improper treatment leading to vulnerability to relapse. DFSP is often superficial; therefore, there are few reports focusing on imaging findings of DFSP.^{3–12} Herein, we provide a retrospective review of the imaging findings of 27 cases of DFSP with the aim to improve our knowledge of DFSP.

MATERIALS AND METHODS

The database of our hospital was searched, and 45 patients with DFSP treated at our hospital were identified between January 2005 and December 2013. Of the 45 patients, 27 patients with complete clinical and imaging data were included in this study and the other 18 patients without complete imaging data were ruled out. An institutional review board exemption and a waiver for the requirement of the written informed consent were obtained to perform this retrospective study.

Of the 27 patients, 18 had been examined with computed tomography (CT) and 9 had undergone magnetic resonance imaging (MRI). CT imaging was performed using a Brilliance TM 16 slices (Philips Medical Systems, Best, The Netherlands) spiral scanner. The scan parameters were as follows: 2 to 5-mm slice thickness reconstructions, 23 to 40-cm field of view, 120 kV voltage, 200 to 300 mA current, and 256 × 256 matrix. An intravenous bolus dose of 100 mL of a nonionic iodinated contrast agent (iopromide; Ultravist; Schering AG, Berlin, Germany) was administered at a rate of 2.5 mL/s to the patients who underwent contrast-enhanced CT. None of the patients were allergic to the iodine contrast medium. Contrast-enhanced CT scans were started 50 to 60 s after the administration of the contrast agent. Contrast-enhanced CT scans were started at 50 to 60 s in 17 cases, whereas multiphase scan was started at 30, 60, and 180 s after the administration of the contrast agent in another 1 case.

MRI was performed using a 1.5-T MRI unit (Signa HDx; GE Healthcare, Milwaukee, WI) and a head and neck or body coil. The MRI protocol included unenhanced axial and coronal T1-weighted sequences, axial and sagittal T2-weighted sequences, and contrast-enhanced axial, sagittal, and coronal T1-weighted sequences. The parameters for these sequences

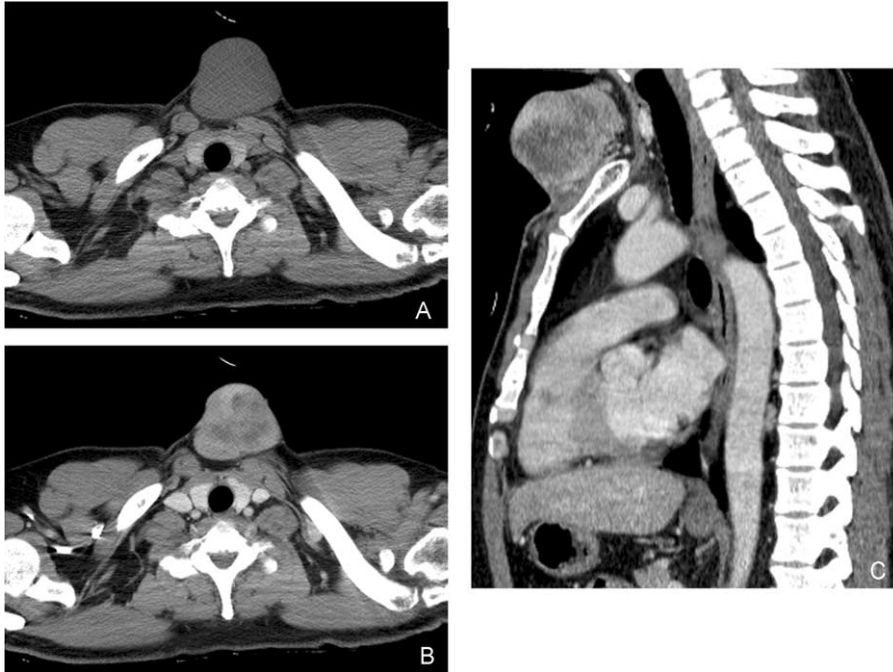


FIGURE 1. Suprasternal fossa tumor. (A) Well-defined homogeneous isodensity on axial unenhanced CT. (B) Intermediate-to-marked heterogeneous enhancement on axial contrast-enhanced CT and (C) multiplanar reconstruction images.

were as follows: T1-weighted spin echo sequence (TR/TE, 530/15 ms; slice thickness, 5.0 mm; field of view, 380–520 mm; matrix scan, 256 × 256) and T2-weighted turbo-spin echo sequence (TR/TE, 4800/120 ms; slice thickness, 5.0 mm; field

of view, 300–380 mm; matrix scan, 256 × 256). An intravenous dose of 0.1 to 0.2 mmol/kg of contrast agent (Gadolinium-DTPA; Magnevist; Schering AG) was administered to the patients undergoing contrast-enhanced MRI.

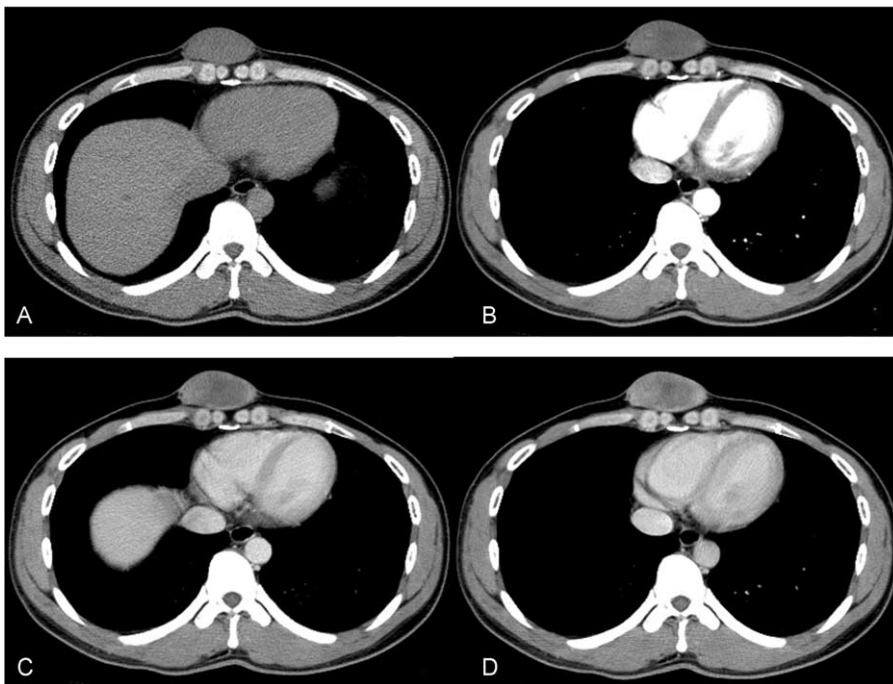


FIGURE 2. Infrasternal fossa tumor. (A) Well-defined homogeneous isodensity on unenhanced CT. (B) Mild heterogeneous enhancement on contrast-enhanced arterial phase CT. (C) Prolonged, delayed enhancement on contrast-enhanced portal venous phase and (D) delayed phase CT.

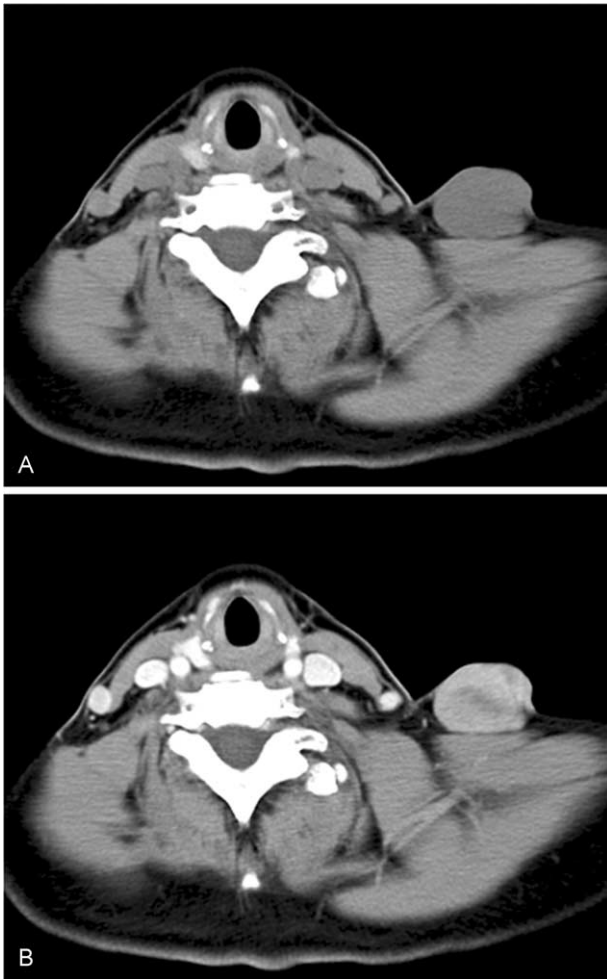


FIGURE 3. Left supraclavicular fossa tumor. (A) Well-defined homogeneous isodensity on unenhanced CT. (B) Intermediate-to-marked heterogeneous enhancement on contrast-enhanced CT.

Two experienced radiologists reviewed the CT and MR imaging characteristics of each lesion, which included location, shape, size, number, edge, and attenuation or intensity of the lesion at unenhanced and contrast enhanced. On unenhanced CT and MR images, attenuation or intensity was classified as hypo, iso, or hyper compared with the adjacent muscle. And after contrast enhancement, the degree of enhancement was classified as no enhancement, mild, moderate, or marked on CT and MR images.

All 27 cases underwent surgery. The histological techniques consisted of routine hematoxylin and eosin (H&E) staining and immunohistochemical evaluation. One pathologist reviewed all the pathological specimens. The macroscopic appearances of each resected tumor were analyzed, including the shape, size, number, edge, and capsule wall. Immunohistochemical analysis included CD34, CD68, desmin, and S-100 protein.

RESULTS

Clinical Data

The study group composed of 15 men and 12 women, with a mean age of 35 years (range, 14–68 years). Of the 27 patients, 24 presented with solitary progressive growing superficial nodules or masses, 2 with 2 nodules, and 1 with multiple nodules. There were 29 lesions in total. Of the 29 lesions, 13 were located in the head and neck and 16 in the trunk. Clinical manifestations were as follows: 24 cases showed painless masses, 2 had a gradual emergence of tingling, and 1 reported feeling of ants biting.

Imaging Findings

The diameter of the tumors ranged from 2 to 17 cm (mean 5.6 cm). One tumor was ill defined and other tumors were well defined. Twenty-five tumors were superficial masses with subcutaneous fat tissue infiltration. There was no evidence of regional lymph node enlargement or bone destruction.

CT Findings

The unenhanced CT images showed 19 homogenous isodense lesions. No calcification was observed in any of the patients. The contrast-enhanced CT images showed intermediate

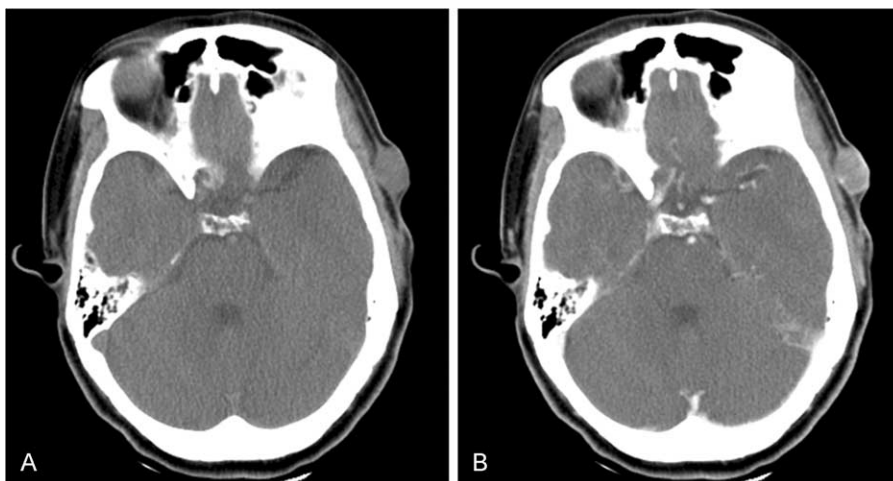


FIGURE 4. Left temporal tumor. (A) Well-defined homogeneous isodensity infiltrating superficial fascia on unenhanced CT. (B) Mild heterogeneous enhancement on contrast-enhanced CT.

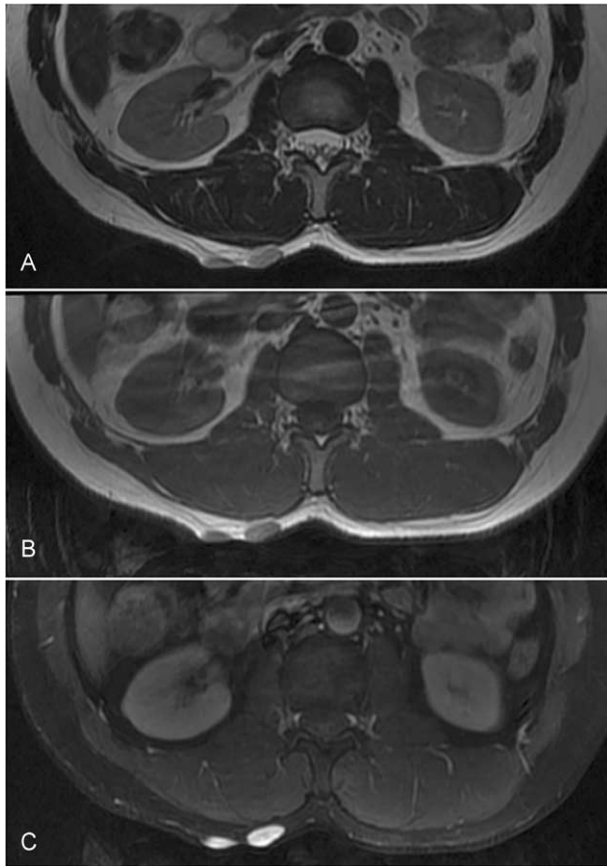


FIGURE 5. Right lower back tumor. (A) Well-defined and homogeneously mild hyperintensity on a T2-weighted MR image. (B) Homogeneously isointensity on a T1-weighted MR image. (C) Heterogeneous hyperintensity on contrast-enhanced fat-suppressed T1-weighted MR image.

and marked heterogeneous enhancement in 13 lesions, intermediate homogeneous enhancement in 4 lesions, and a mild heterogeneous enhancement in 2 lesions (Figures 1–4).

MRI Findings

MR T1-weighted images revealed 9 well-defined homogeneous isointense or mild hyperintense lesions. T2-weighted images showed homogeneous hyperintensity to the muscles for 6 lesions and 3 mild hyperintense foci with hypointense masses. In 1 case with a multiple confluent frontal scalp lesion, the tumor showed ill-defined isointensity on T1-weight images, and mixed, mild hyperintensity and isointensity on T2-weighted images. Contrast-enhanced T1-weighted images demonstrated intermediate and marked nonhomogeneous enhancement in 9 lesions and intermediate homogeneous enhancement in 1 mass (Figures 5–7).

Follow-Up

No cases showed distant metastasis at diagnosis. Twenty-five cases showed no recurrence during 6 months to 3 years of follow-up. Two cases were lost at follow-up.

Histopathology

Tumors composed of uniform spindle cells with long or short spindle nuclei. Spindle cells were arranged in a dense

striated form. Mitosis was not common. Varying amounts of the collagen were visible in parts of the interstitial tissue. The immunohistochemical results demonstrated that all cases were CD34⁺ (Figure 8). CD68 was positive in 18 cases, and desmin and S-100 protein were negative for 25 and 24 cases, respectively.

DISCUSSION

DFSP is a rare, low-grade, locally aggressive neoplasm, accounting for approximately 6% of soft tissue sarcomas. In the 2013 World Health Organization classification of soft tissue and bone tumors, DFSP was classified as a fibroblastic/myofibroblastic tumor.¹³ DFSP has several variants, such as pigmented, myxoid, granular cell, sclerosing DFSP, and DFSP with areas of giant cell fibroblastoma.¹⁴ Genetically, DFSP is characterized by the t(17; 22)(q22; q13) translocation, which leads to a fusion of the α -chain type 1 of collagen gene and platelet-derived growth factor β gene. This reciprocal translocation is present in 90% of DFSP cases.^{13,14} Histologically, DFSP often appears as a poorly circumscribed tumor, which infiltrates the dermis and subcutis diffusely. Tumors composed of uniform spindle cells with elongated nuclei arranged in an interwoven fascicular storiform or cartwheel pattern, embedded in varying amounts of collagen. Mitotic activity is often low. Immunohistochemically, CD34 is positive in 90% of DFSP patients, which is often used to differentiate DFSP from other tumors.^{13,14} In our study, all cases were CD34⁺.

DFSP is more common in adults between 20 and 50 years.¹³ Its slow growth suggests that the tumor could arise in childhood. There is no sex bias.¹⁵ In this study, 2 patients were <20 years, 1 was 68 years old, and the remaining were between 20 and 60 years, which is similar to the previous reports. DFSP can occur in almost any part of the body, the most common site is the trunk, followed by proximal extremities; head and neck are less common.^{13,15} However, in our study, trunk cases accounted for 55% of all cases, and head and neck cases accounted for 45%, which perhaps reflects our small sample.

DFSP grows slowly, ranging from several months to many years, starting in an indurate plaque, mostly reddish brown or light blue, later developing into a nodule in the plaque.¹⁴ DFSP often demonstrates round, oval, or irregular soft tissue nodule or mass, and protrudes skin surfaces to different degrees. The tumor is usually solitary and relapsed cases often show lobulated or multiple nodules. The tumor borders are frequently clear, and cysts and bleeding are rare.

On ultrasound, DFSP showed a low echo mass with a rich blood supply.^{10,16} On CT, DFSP often showed a solitary, well-defined isodense cutaneous or subcutaneous nodule or mass, with no calcification. DFSP showed homogeneous enhancement for small tumors and nonhomogeneous enhancement for large tumors.^{4–6} The tumors are slow growing; therefore, the tumor often is large when patients are referred for CT or MRI. In the report by Li et al⁶, 15 out of 17 lesions that underwent CT scans were well defined, and 12 lesions showed moderate or marked homogeneous enhancement. In our study, 19 lesions appeared as solitary well-defined isodense masses, and no lesions showed calcification on an unenhanced CT scan. After contrast injection, 13 lesions showed moderate and marked nonhomogeneous enhancement, 2 lesions showed mild nonhomogeneous enhancement, whereas the remaining 4 masses showed intermediate homogeneous enhancement. In our study, 1 case underwent body multiple-phase CT scan, and the lesions

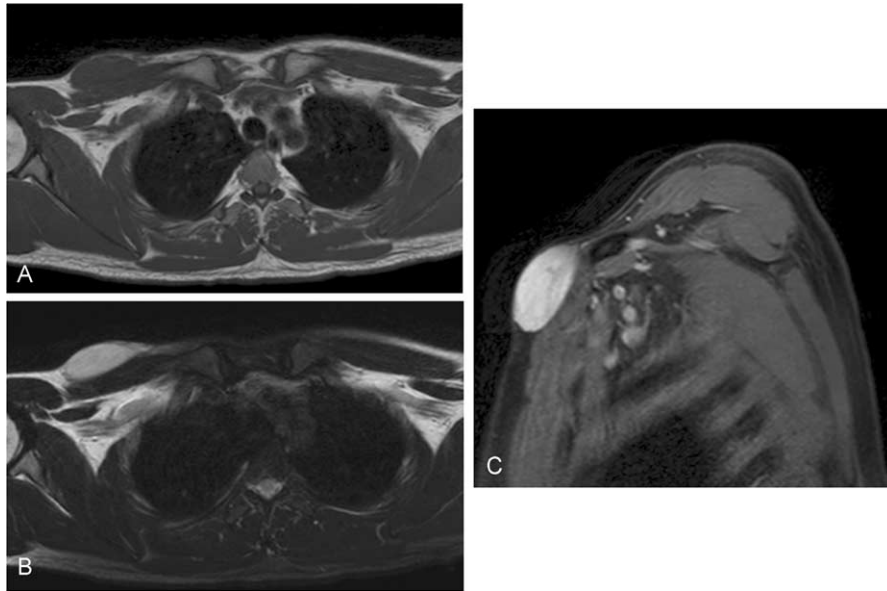


FIGURE 6. Left supraclavicular fossa tumor. (A) Well-defined and homogeneous isointensity on a T1-weighted MR image. (B) Homogeneously intermediate hyperintensity on a T2-weighted MR image. (C) Homogeneous hyperintensity on a contrast-enhanced fat-suppressed T1-weighted MR image.

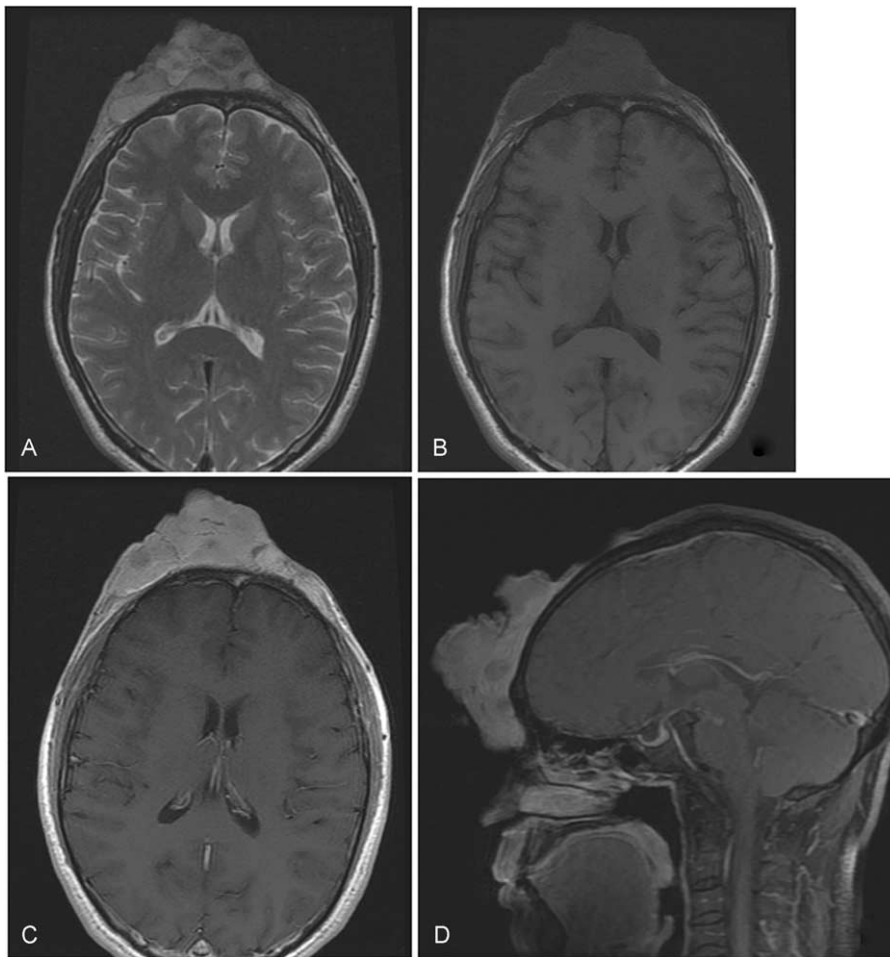


FIGURE 7. Frontal scalp tumor. (A) Ill-defined and heterogeneously mild hyperintensity and isointensity on a T2-weighted MR image. (B) Isointensity on a T1-weighted MR image. (C, D) Heterogeneous hyperintensity on contrast-enhanced T1-weighted MR images.

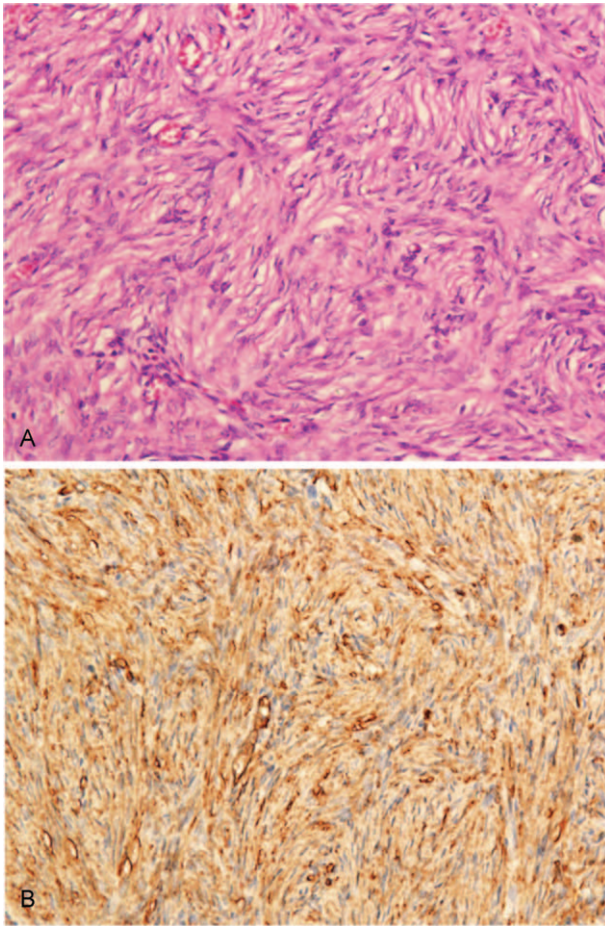


FIGURE 8. DFSP specimen with typical histopathological features showing spindle cells in storiform arrangement. The cells stain positive for CD34. (A) H&E and (B) immunohistochemical stain; original magnification $\times 200$. DFSP = dermatofibrosarcoma protuberans, H&E = hematoxylin and eosin.

showed mild-to-intermediate prolonged, delayed enhancement. The prolonged enhancement areas may have correlated with abundant hypercellular areas, and the delayed enhancement may have correlated with collagen tissue.¹⁷

On MRI, the tumor often appeared as a well-defined isointense nodule or mass compared with muscle on T1-weighted images, and was hyperintense on T2-weighted images. On contrast-enhanced T1-weighted images, the tumor demonstrated intermediate or marked homogeneous or heterogeneous enhancement.^{8–10} In most cases, the tumor was homogeneous intense. In some cases, there were necrotic and hemorrhagic signals on MRI.⁴ In our study, 9 lesions demonstrated well-defined homogeneous isointense masses on T1-weighted images, and intermediate or mild hyperintense on T2-weighted images. On contrast-enhanced T1-weighted images, the tumor showed intermediate and marked heterogeneous enhancement. DFSP is often rich in blood supply.^{4,16} In the report by Kransdorf and Meis-Kindblom⁴, 1 case underwent angiography, which showed a large number of tumor vessels. Thus, DFSP often demonstrates intermediate-to-marked enhancement. By contrast, there were some areas showing no enhancement in 2 lesions in our study; we speculated that they

might have resulted from cystic and necrotic areas, which is similar to previous reports.¹⁷ The mild enhancement in parts of the tumor might have been caused by collagen tissue in the tumor stroma. In our study, 1 case showed an ill-defined confluent mass, which is rare in primary cases but frequently observed in relapsed cases.

DSFP is often superficial, and has typical clinical manifestations. In routine clinical work, MRI is not the first choice. However, DFSP could infiltrate into the dermis and subcutaneous tissues, extending far beyond the clinical margins. In the report by Garg et al,⁷ a DFSP arising in the leg showed contiguous infiltration of the underlying bone. In another report by Thornton et al,⁸ the proposed surgical margins were enlarged relying on the MR imaging findings in 2 out of 5 cases. Thus, presurgical MRI is important for surgical plan and follow-up.

The prognosis of DFSP is generally good. Surgical resection is the main treatment for DFSP. However, DFSP has a high rate of local recurrence, but little distant metastasis.⁴ With simple tumor resection, the mean recurrence rate is approximately 20%, whereas with Mohs micrographic surgery, the recurrence rate is $<1\%$.¹⁴ Thus, postoperative follow-up is particularly important, especially in the first 3 years.¹⁸ In our study, no case showed distant metastasis at initial diagnosis, and 25 out of 27 cases showed no recurrence and metastasis from 6 months to 3 years of follow-up.

The imaging findings for DFSP are nonspecific; however, it needs to be differentiated from other diseases, such as lipoma, liposarcoma, dermatofibroma, neurogenic tumor, and hemangioma. Lipoma and liposarcoma often occur in the subcutaneous tissue of limbs. The tumor shows fat density on CT, and high signal, both on T1- and T2-weighted images, and is only enhanced a little on enhanced images. On the MRI fat suppression sequence, the tumor shows a low signal. Dermatofibroma, whether single or multiple, occurs in various parts of the limbs, accompanied by thickening of the skin tissue.³ Neurogenic tumors include schwannomas and neurofibromas, which grow mainly along nerves. Schwannoma often shows cystic degeneration heterogeneous enhancement. Hemangioma often occurs in the limb muscles and is a painless soft tissue mass, which shows calcification on CT, isointense on T1-weighted images, and hyperintense on T2-weighted images with dots or lines of low signal, which signifies calcification or venous stones, and centric enhancement is observed on enhanced images.^{19,20}

Our study is a single-site, retrospective analysis. Our sample size was relatively small; therefore, the distribution of DFSP lesion locations might have been biased. In our study, head and neck cases accounted for 45%, which is different from other studies. However, the DFSP imaging findings of different locations in this study were similar, which is in keeping with published reports.^{6–11}

In conclusion, DFSP is characterized by a subcutaneous well-defined soft tissue nodule or mass on plain CT/MR scans, and shows intermediate-to-marked enhancement on contrast-enhanced CT/MR scans. The imaging findings for DFSP are nonspecific, but may help to define the diagnosis in an appropriate clinical setting.

REFERENCES

1. Darier J, Ferrand M. Dermatofibromes progressifs et recidivants ou fibrosarcomes de la peau. *Ann Dermatol Syphiliga*. 1924;5:545–562.
2. Hoffman E. Ueber das knollentribende fibrosarkam der haut (dermatofibrosarcoma protuberans). *Dermatol Z*. 1925;43:1–28.

3. Millare GG, Guha-Thakurta N, Sturgis EM, et al. Imaging findings of head and neck dermatofibrosarcoma protuberans. *AJNR Am J Neuroradiol*. 2014;35:373–378.
4. Kransdorf MJ, Meis-Kindblom JM. Dermatofibrosarcoma protuberans: radiologic appearance. *AJR Am J Roentgenol*. 1994;163:391–394.
5. Miyakawa E, Fujimoto H, Miyakawa K, et al. Dermatofibrosarcoma protuberans. CT findings with pathologic correlation in 6 cases. *Acta Radiol*. 1996;37:362–365.
6. Li X, Zhang W, Xiao L, et al. Computed tomographic and pathological findings of dermatofibrosarcoma protuberans. *J Comput Assist Tomogr*. 2012;36:462–468.
7. Garg MK, Yadav MK, Gupta S, et al. Dermatofibrosarcoma protuberans with contiguous infiltration of the underlying bone. *Cancer Imaging*. 2009;9:63–66.
8. Thornton SL, Reid J, Papay FA, et al. Childhood dermatofibrosarcoma protuberans: role of preoperative imaging. *J Am Acad Dermatol*. 2005;53:76–83.
9. Torreggiani WC, Al-Ismaïl K, Munk PL, et al. Dermatofibrosarcoma protuberans: MR imaging features. *AJR Am J Roentgenol*. 2002;178:989–993.
10. Bergin P, Rezaei S, Lau Q, et al. Dermatofibrosarcoma protuberans, magnetic resonance imaging and pathological correlation. *Australas Radiol*. 2007;51:B64–B66.
11. Liu SZ, Ho TL, Hsu SM, et al. Imaging of dermatofibrosarcoma protuberans of breast. *Breast J*. 2010;16:541–543.
12. Gatlin JL, Hosch R, Khan M. Dermatofibrosarcoma protuberans of the scalp with fibrosarcomatous degeneration and pulmonary metastasis. *J Clin Imaging Sci*. 2011;1:55.
13. Fletcher CDM, Bridge JA, Hogendoorn PCW, et al. World Health Organization classification of tumours. *Pathology and Genetics of Tumours of Soft Tissue and Bone*. Lyon, France: IARC Press; 2013 77–79.
14. Llombart B, Serra-Guillén C, Monteagudo C, et al. Dermatofibrosarcoma protuberans: a comprehensive review and update on diagnosis and management. *Semin Diagn Pathol*. 2013;30:13–28.
15. Bogucki B, Neuhaus I, Hurst EA. Dermatofibrosarcoma protuberans: a review of the literature. *Dermatol Surg*. 2012;38:537–551.
16. Djilas-Ivanovic D, Prvulovic N, Bogdanovic-Stojanovic D, et al. Dermatofibrosarcoma protuberans of the breast: mammographic, ultrasound, MRI and MRS features. *Arch Gynecol Obstet*. 2009;280:827–830.
17. Zhang WD, Chen JY, Cao Y, et al. Computed tomography and magnetic resonance imaging findings of solitary fibrous tumors in the pelvis: correlation with histopathological findings. *Eur J Radiol*. 2011;78:65–70.
18. Archontaki M, Korkolis DP, Arnogiannaki N, et al. Dermatofibrosarcoma protuberans: a case series of 16 patients treated in a single institution with literature review. *Anticancer Res*. 2010;30:3775–3779.
19. Walker EA, Salesky JS, Fenton ME, et al. Magnetic resonance imaging of malignant soft tissue neoplasms in the adult. *Radiol Clin North Am*. 2011;49:1219–1234.
20. Walker EA, Fenton ME, Salesky JS, et al. Magnetic resonance imaging of benign soft tissue neoplasms in adults. *Radiol Clin North Am*. 2011;49:1197–1217.